TECHNICAL NOTE

D-834

TRANSONIC INVESTIGATION OF AERODYNAMIC CHARACTERISTICS OF A SWEPT-WING FIGHTER-AIRPLANE MODEL WITH LEADING-EDGE DROOP IN COMBINATION WITH OUTBOARD CHORD-EXTENSIONS AND NOTCHES

By Charles F. Whitcomb and Harry T. Norton, Jr.

Langley Research Center
Langley Field, Va.

NATIONAL AERONAUTICS AND SPACE ADMINISTRATION
WASHINGTON May 1961

NATIONAL AERONAUTICS AND SPACE ADMINIS

TECHNICAL NOTE D-834

TRANSONIC INVESTIGATION OF AERODYNAMIC CHARACTERISTICS OF A SWEPT-WING FIGHTER-AIRPLANE MODEL WITH LEADING-EDGE DROOP IN COMBINATION WITH OUTBOARD CHORD-EXTENSIONS AND NOTCHES[1]

By Charles F. Whitcomb and Harry T. Norton, Jr.

SUMMARY

An investigation of the effects of several wing leading-edge modifications on the aerodynamic characteristics of a 45° swept-wing fighter-airplane model has been conducted in the Langley 16-foot transonic tunnel at low and high lifting conditions at Mach numbers from 0.85 to 1.03. The investigation included the determination of the effect on longitudinal stability and performance characteristics of wing leading-edge and chord-extension droops of 6° and 20°, chord-extension overhangs of 0.075c and 0.15c (where c is the wing chord), leading-edge notches cut out at the inboard end of the 0.075c chord-extension to depths of 0.075c and 0.125c, and indention of the model fuselage to conform partially to the supersonic area rule for a Mach number of 1.20. Lift, drag, and pitching-moment data were obtained for configurations with the tail on and off. Comparisons of data obtained from the present model with data from a configuration with leading-edge slats are included.

Generally, the model wing modifications provided only slight improvement of the airplane longitudinal stability characteristics, but did substantially reduce the airplane drag coefficients at moderate and high lifting conditions.

INTRODUCTION

The loss of longitudinal stability and the high values of drag due to lift at the higher lifting conditions are two adverse characteristics of airplanes with thin, swept wings of low aspect ratio operating at transonic speeds. Improvement of these characteristics, in particular the instability, was realized at low subsonic speeds by using modifications such as leading-edge droop, outboard leading-edge chord-extensions, leading-edge slats, and leading-edge notches combined with leading-edge extensions

[1]Supersedes declassified NACA Research Memorandum L55H30 by Charles F. Whitcomb and Harry T. Norton, Jr., 1956.

(refs. 1 and 2). However, the effectiveness of these devices was considerably reduced at the higher subsonic and transonic speed ranges (refs. 3, 4, and 5).

An investigation was conducted by the NACA to determine the effectiveness of leading-edge slats on the high subsonic and transonic aerodynamic characteristics of a 45° swept-wing fighter airplane. The results of that investigation are presented in reference 5. To broaden the scope of that program, several other configurations of general interest which included wing leading-edge droop in combination with outboard leading-edge chord-extensions and leading-edge notches were included for testing over the same speed range. The results of tests of these configurations, primarily selected to improve the airplane longitudinal stability, are presented in this paper.

L
1
0
6
0

The basic model was a fighter-type airplane having a wing plan-form geometry (45° sweepback and aspect ratio of 3.56) that made it inherently unstable at the higher lifts. (See ref. 6.) The investigation was conducted in the Langley 16-foot transonic tunnel at Mach numbers from 0.85 to 1.03, and at angles of attack from 0° to 20°. The models tested included tail-on and tail-off configurations. Some of the results of reference 5 are included for comparison with the present test results.

SYMBOLS

$b/2$	wing semispan
C_D	drag coefficient, D/qS
C_L	lift coefficient, L/qS
C_m	pitching-moment coefficient, $\dfrac{\text{Pitching moment about } 0.35\bar{c}}{qS\bar{c}}$
c	local wing chord
$\bar{c}$	basic wing mean aerodynamic chord
D	drag
L	lift
M	free-stream Mach number
l_t	tail length

C_{p_B} base pressure coefficient, $\frac{p_B - p}{q}$

p free-stream static pressure

p_B static pressure at model base

q free-stream dynamic pressure

R Reynolds number based on $\bar{c}$

L
1
0
6
0

S basic wing area

α angle of attack of fuselage reference line

δ_h incidence of horizontal tail with respect to fuselage reference line

Subscripts:

Basic basic wing (no leading edge modification)

E leading-edge extension

max maximum

MODEL AND APPARATUS

Tunnel

The investigation was conducted in the Langley 16-foot transonic wind tunnel, the airflow and power characteristics of which are described in reference 7. The model was attached to the tunnel sting-support system by means of a six-component internal strain-gage balance.

Basic Model

The basic model is the same as that used in reference 5. The basic wing has 45° sweepback along the 0.25-chord line, taper ratio of 0.3, aspect ratio of 3.56, and NACA $64_{(06)}$A007 airfoil sections parallel to the plane of symmetry. The vertical and horizontal tails have essentially the same geometry as the wings. The horizontal tail was located 0.03 of the tail length below the wing-chord plane extended and the horizontal-tail incidence was -5° for all tail-on tests. Tail-off configurations include

the removal of both the horizontal and vertical tails. The canopy, tail fillet, faired-nose section, and wing leading-edge section from the 0.20-chord line forward were constructed of wood; the remainder of the model was fabricated from aluminum alloy. A detailed listing of dimensions for the basic model is presented in table I of reference 5. Figure 1 is a photograph of the complete basic model and a photograph of the model with 20° drooped-wing leading edge and 0.15 chord-extension. A three-view drawing of the model showing a typical configuration of a leading-edge chord-extension with notch is shown in figure 2.

Model Modifications

Two angles of droop, 6° and 20°, were investigated, the angle being measured normal to the wing 0.20-chord line. The forward 20 percent of the airfoil sections from $0.25\frac{b}{2}$ to $1.00\frac{b}{2}$ was drooped along a straight camber line.

The leading-edge chord-extension was designated by the percent of chord-extension at the station of the inboard end of the extension, $0.71\frac{b}{2}$, and was tapered to zero-percent chord at the wing tip. Droop of the chord-extensions was also measured normal to the basic wing 0.20-chord line. The 0.075c chord-extensions with 6° droop and the 0.15c chord-extensions with 6° and 20° droop were tested.

Notches in the wing leading edge extending from wing station 0.69 to $0.71\frac{b}{2}$, the inboard end of the chord-extension, were tested in combination with the 0.075c chord-extensions and 6° droop. Notches with a depth of 0.075c and 0.125c were investigated.

The indented body used in these tests was the identical body used in the transonic drag-rise investigation of reference 8. It was obtained for that investigation by recontouring the basic fuselage according to supersonic-area-rule considerations for a Mach number of 1.2.

TESTS AND CORRECTIONS TO DATA

The nine model configurations tested are listed in the following table:

Wing	Chord-extension	Notch	Tail	Body
Basic	None	None	Off	Basic
6° leading-edge droop	0.075c	None	Off	Basic
6° leading-edge droop	.075c	0.075c	Off	Basic
6° leading-edge droop	.075c	.125c	Off	Basic
6° leading-edge droop	.15c	None	Off	Basic
6° leading-edge droop	.15c	None	On	Basic
20° leading-edge droop	.15c	None	Off	Basic
20° leading-edge droop	.15c	None	On	Basic
6° leading-edge droop	.15c	None	On	M = 1.2 indented

The configurations were tested through an angle-of-attack range of 0° to 20° for Mach numbers from 0.85 to 0.97, and 0° to 12° for Mach numbers 1.00 and 1.03. Test Reynolds numbers, shown in figure 3, varied from 5.65×10^{6} to 6.75×10^{6} based on the basic wing mean aerodynamic chord.

The model lift and drag data were adjusted to a condition of free-stream static pressure at the base of the fuselage using base pressures averaged from three static orifices spaced equidistantly around the base annulus just inside the duct of the model. The variation of base pressure with Mach number is shown in figure 4. As the sting-interference effects for the tail-off configurations were known to be small and any sting interference on the tail-on configurations would be about the same for each of the compared configurations, no corrections for this effect were considered necessary. Tunnel-wall interferences are neglected in the Mach number range considered in this paper (ref. 9).

The accuracy of the measured coefficients, based on balance accuracy and repeatability of data, is believed to be within the following limits:

C_L . . . . . ±0.01
C_D . . . . . ±0.002
C_m . . . . . ±0.002

The accuracy of Mach number is ±0.005 and the angles of attack as presented are estimated to be accurate to ±0.1°.

RESULTS

The results of the investigation are presented graphically as follows:

DISCUSSION

Longitudinal Stability

Figures 5(c) and 6(c) present the variation of pitching-moment coefficient with lift coefficient for several tail-off configurations tested. The basic model exhibited unstable breaks at all Mach numbers for moderate lifting conditions. Addition of any of the several leading-edge devices tested generally resulted in a more gradual change in the stability curves and an extension of the stable lift range up to a 0.15 increment in lift coefficient, depending on which configuration and Mach number range is considered. The extensions of the stable lift ranges for the present configurations were considerably less than anticipated on the basis of the results of reference 4, which reports on tests of several of the same types of wing modifications on a wing very similar to the present model.

A comparison of several modified configurations with tail off indicates that neither the addition of the notches (either 0.075c or 0.125c deep) nor the lengthening of the chordwise extent (0.075c to 0.15c) of the configuration with a 6° drooped chord-extension improved the stability characteristics any significant amount. However, reference 10 indicated that a similar change in the chordwise length of the extensions without notches resulted in a significant improvement in stability. The inboard end of the chord-extensions in reference 10 was located at 65-percent wing semispan as compared with 71-percent semispan for the present tests. As the optimum span of chord-extensions in the transonic range is believed to be a critical function of wing plan-form geometry, it appears that the inboard ends of the configurations tested here were located too far outboard. As a result the test changes or effective changes (such as adding notches) in the chordwise direction were not as effective in influencing the tip separation characteristics of the wing as was the change made in reference 10.

L
1
0
6
0

Increasing the droop angle from 6° to 20° for the configuration with a 0.15c extension had no consistent effect on the stability of the configuration, but at Mach numbers of 0.93 and 0.95 (fig. 5(c)) there was a significant increase in the longitudinally stable lift range.

The stability results of the three modified configurations with tail on as obtained from the present tests are compared with the basic-model results of reference 5 in figure 7(c). The horizontal-tail incidence was set the same as in reference 5 ($\delta_h = -5^\circ$). Also, the vertical position of the horizontal tail below the wing-chord plane extended was the same, and is a position that should make a large contribution to the stability of the basic model at high lifts (ref. 11). The comparisons indicated no significant stability improvement contributed by the configuration with a 6° drooped wing chord-extension above a Mach number of 0.85, at which Mach number the unstable pitching-moment reversals were essentially eliminated. Increasing the droop from 6° to 20° did not delay the breaks to higher lift coefficients, but reduced their severity a significant amount. At a Mach number of 0.95 the curve reversals were reduced to slight inflections at a lift coefficient of 0.6.

In addition to the preceding changes in wing geometry, drag-reducing indentations in the body were also believed to contribute to the control of premature wing-tip separation (ref. 12). Revisions of longitudinal area distribution of the model, based on area-rule concepts, are designed to reduce the intensity of the model deceleration wave which intersects the swept wing tip at Mach numbers of about 0.90. Such reduced wave intensity should alleviate any wing-flow separation directly associated with it. The configuration with a $M = 1.2$ indented body of reference 8, adapted with 6° leading-edge droop and 0.15c chord-extension wing modifications, was tested at high lifting conditions to investigate this possibility.

The pitching-moment results presented in figure 7(c) indicate that only for a Mach number of 0.90 does the indented body benefit the model stability characteristics. At this Mach number the severity of the unstable slope reversal was decreased.

The pitching-moment characteristics of the model modified with 20° wing leading-edge droop and 0.15c chord-extensions are compared at several Mach numbers (fig. 8) with the results obtained in reference 5 for the present model with 0.46 to $0.95\frac{b}{2}$ wing leading-edge slats. The 0.46 to $0.95\frac{b}{2}$ slat span was the more effective of the two slat spans tested in improving longitudinal stability. Comparisons are made for both tail-on and tail-off models. The slat droop angle was 10°. The difference in droop angle and in spanwise extension make direct comparisons somewhat difficult, especially since the chord-extension span is believed to be too short. However, the use of the same basic model does eliminate the test vehicle geometry variables, and comparison of this slat configuration with what was essentially the most effective of the chord-extension configurations tested would be of some interest.

L
1
0
6
0

The pitching-moment-curve breaks of the slat configuration with tail off are of more gradual nature than those of the configuration with drooped leading-edge chord-extension up to lift coefficients of approximately 0.70. With the addition of the tail to the model, the stable lift range of the slat configuration was extended well above that of the drooped-extension configuration at Mach numbers of 0.90 and 0.93. At the high Mach numbers of 0.95 and 0.97, the configuration with 20° drooped extension had stability characteristics comparable with those produced by the slat configuration.

Lift Characteristics

The results of adding the several leading-edge devices to the basic-wing model with tail off are presented in figures 5(a) and 6(a). The increases in lift for the various leading-edge devices are attributed to the droop of the leading edge in each case. The lift was significantly increased above angles of attack of approximately 12° by increasing the leading-edge droop from 6° to 20°. There were no large differences in lift characteristics with other modifications. The results for the tail-on model were essentially the same as for the tail-off model (fig. 7(a)).

Drag Characteristics

All wing modifications for the tail-off model, with the exception of the configuration with 6° drooped leading-edge and 0.15c extension, decreased the drag above lift coefficients of 0.60 and slightly increased the drag at zero and low lifts. (See figs. 5(b) and 6(b).) For the configuration with 6° drooped leading-edge and 0.15c chord-extension, the drag was lower than for the basic model at zero and low lift conditions at Mach numbers from 0.93 to 1.03. It is believed that the major portion of these differences can be attributed to instrument accuracy and data-repeatability limitations. The changes in the various leading-edge devices had little effect on the drag characteristics. However, the slight changes that did occur can be attributed to increasing the leading-edge droop from 6° to 20°.

For the tail-on model, increasing the leading-edge droop from 6° to 20° with the 0.15c extension caused drag changes similar to those for the tail-off configurations (fig. 7(b)). Indenting the body of the configuration with 6° drooped leading edge and 0.15c extension resulted in reduced drag at low lifts for Mach numbers above 0.90 (fig. 7(b)).

Lift-Drag Ratio Characteristics

The maximum lift-drag ratios for several of the configurations tested are presented in figure 9. Results from the tests of the configurations with notched wing were not included, since it is evident from the drag polars of figure 6(b) that these results would indicate no significant change from those of the basic chord-extension configuration. For all the revised-wing configurations with tail off, the $(L/D)_{max}$ values are less than those of the basic-wing configurations over the entire test Mach number range. For each of the modified configurations, $(L/D)_{max}$ occurs at a lift coefficient somewhat lower than that at which the drag polars of the modified models show a drag reduction below that of the basic model. Relative to the absolute values of the parameter, the decrements are not considered large, except those obtained from the configuration with 20° drooped leading edge and 0.15c extension. Of the tail-on configurations presented, some slight increases in $(L/D)_{max}$ values above the drag-rise Mach number are attributed to the $M = 1.2$ drag-reducing indentations of the basic fuselage.

The ratios of L/D obtained from the various revised-wing configurations with tail off to L/D for the basic-wing configuration are presented as a function of lift coefficient in figure 10. Gains in L/D above the basic model (or decreased drags due to lift) are indicated for each of the revised-wing configurations. The improvements occurred above

lift coefficients ranging from 0.2 to 0.65, depending on the Mach number and particular device under consideration. (The notched-wing information has again been omitted.) Increasing the chordwise length of the 6° drooped leading-edge extension from 7.5 to 15 percent resulted in only small changes in L/D, but increasing the droop angle from 6° to 20° produced significant effects. The configuration with leading-edge chord-extensions drooped 20° showed improved performance over the 6° drooped configuration at the higher lift coefficients only. Any advantages relative to the configurations with lower droop angle were limited in lift range to values above $C_L = 0.65$ at Mach numbers of 0.85 to 0.93 and above $C_L = 0.80$ at the higher Mach numbers. From this indication, it would seem advisable to consider variable leading-edge droop where such devices are being incorporated.

L
1
0
6
0

For an additional comparison, the L/D values derived from the results presented in reference 5 for the present test model with a 0.35 to $0.95\frac{b}{2}$ leading-edge-slat wing with tail off are presented in figure 11. From performance considerations the 0.35 to $0.95\frac{b}{2}$ slat span was the more effective of the two slat lengths tested. Comparison is made of the configuration with 10° drooped slats and the configuration with 20° drooped wing leading edge and 0.15c extension at several Mach numbers. The good agreement at the presented conditions may indicate that introducing a slat gap along the leading edge has the same effects on the wing aerodynamic characteristics as increasing the wing leading-edge camber.

CONCLUDING REMARKS

A transonic investigation of several configurations with leading-edge droop in combination with outboard chord-extensions and notches as adapted to a swept-wing fighter-airplane model indicated that their application provided only slight improvement of the airplane longitudinal stability characteristics. However, the airplane drag coefficients were substantially reduced at moderate and high lifting conditions.

Langley Aeronautical Laboratory,
National Advisory Committee for Aeronautics,
Langley Field, Va., August 17, 1955.

L
1
0
6
0

REFERENCES

1. Furlong, G. Chester, and McHugh, James G.: A Summary and Analysis of the Low-Speed Longitudinal Characteristics of Swept Wings at High Reynolds Number. NACA Rep. 1339, 1957. (Supersedes NACA RM L52D16.)

2. Weil, Joseph, and Morrison, William D., Jr.: A Study of the Use of Leading-Edge Notches as a Means for Improving the Low-Speed Pitching-Moment Characteristics of a Thin 45° Swept Wing of Aspect Ratio 4. NACA RM L53J27a, 1953.

3. West, F. E., Jr., Liner, George, and Martz, Gladys S.: Effect of Leading-Edge Chord-Extensions on the Aerodynamic Characteristics of a 45° Sweptback Wing-Fuselage Combination at Mach Numbers of 0.40 to 1.03. NACA RM L53B02, 1953.

4. Spreemann, Kenneth P., and Alford, William J., Jr.: Investigation of the Effects of Leading-Edge Chord-Extensions and Fences in Combination With Leading-Edge Flaps on the Aerodynamic Characteristics at Mach Numbers From 0.40 to 0.93 of a 45° Sweptback Wing of Aspect Ratio 4. NACA TN 3845, 1957. (Supersedes NACA RM L53A09a.)

5. Runckel, Jack F., and Schmeer, James W.: The Aerodynamic Characteristics at Transonic Speeds of a Model With a 45° Sweptback Wing, Including the Effect of Leading-Edge Slats and a Low Horizontal Tail. NACA RM L53J08, 1954.

6. Weil, Joseph, and Gray, W. H.: Recent Design Studies Directed Toward Elimination of Pitch-Up. NACA RM L53I23c, 1953.

7. Ward, Vernon G., Whitcomb, Charles F., and Pearson, Merwin D.: Air-Flow and Power Characteristics of the Langley 16-Foot Transonic Tunnel With Slotted Test Section. NACA RM L52E01, 1952.

8. Whitcomb, Charles F., and Lee, Edwin E., Jr.: Drag Investigation of a Swept-Wing Fighter-Airplane Model Incorporating Two Drag-Rise-Reducing Fuselage Revisions. NACA RM L55E24, 1955.

9. Whitcomb, Charles F., and Osborne, Robert S.: An Experimental Investigation of Boundary Interference on Force and Moment Characteristics of Lifting Models in the Langley 16- and 8-Foot Transonic Tunnels. NACA RM L52L29, 1953.

10. Goodson, Kenneth W., and Few, Albert G., Jr.: Effect of Leading-Edge Chord-Extensions on Subsonic and Transonic Aerodynamic Characteristics of Three Models Having 45° Sweptback Wings of Aspect Ratio 4. NACA RM L52K21, 1953.

11. Morrison, William D., Jr., and Alford, William J., Jr.: Effects of Horizontal-Tail Height and a Wing Leading-Edge Modification Consisting of a Full-Span Flap and a Partial-Span Chord-Extension on the Aerodynamic Characteristics in Pitch at High Subsonic Speeds of a Model With a 45° Sweptback Wing. NACA RM L53E06, 1953.

12. West, F. E., Jr., and Henderson, James H.: Relationship of Flow Over a 45° Sweptback Wing With and Without Leading-Edge Chord-Extensions to Longitudinal Stability Characteristics at Mach Numbers From 0.60 to 1.03. NACA RM L53H18b, 1953.

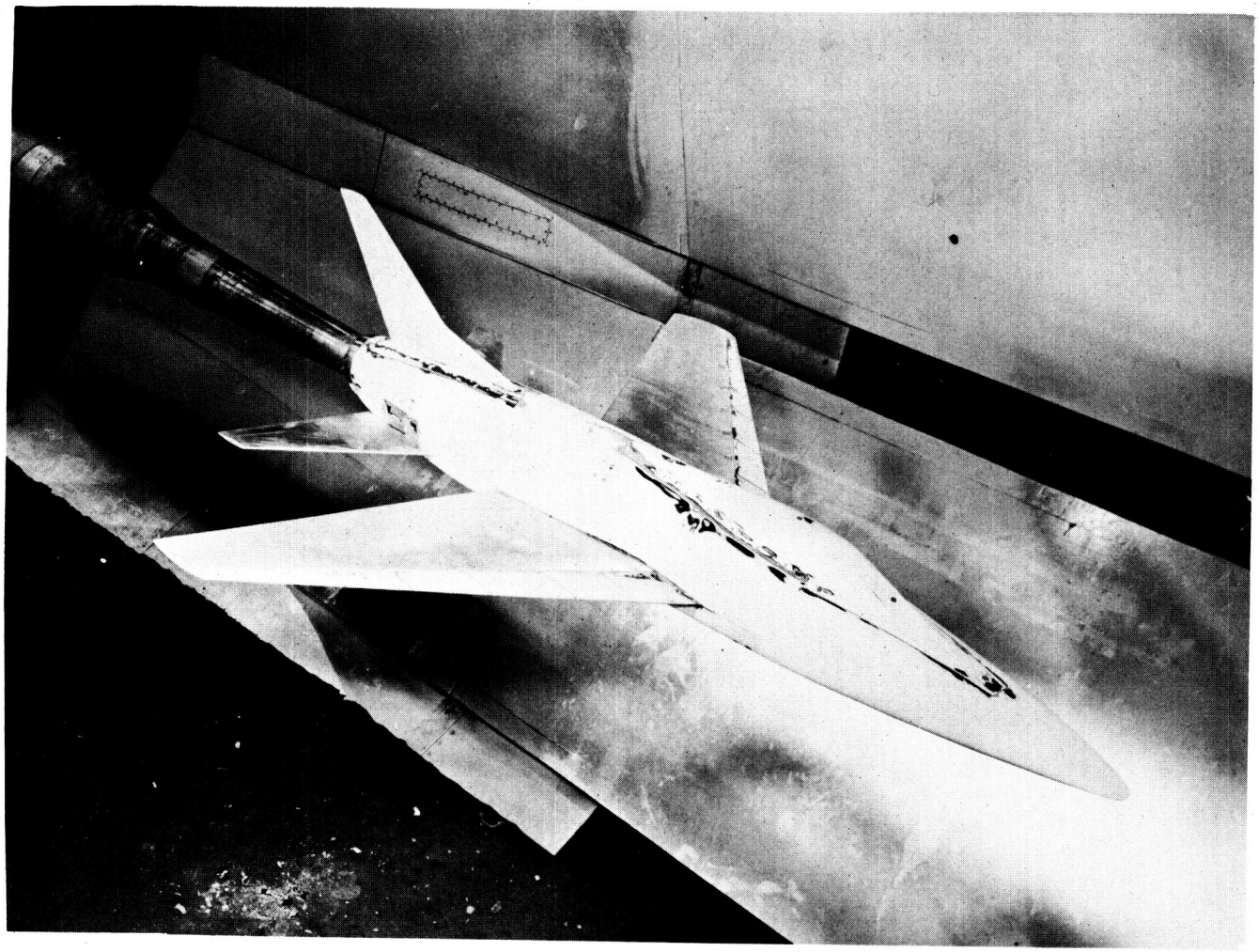

(a) Complete model with basic-wing configuration. L-82817

Figure 1.- Model in Langley 16-foot transonic tunnel.

L-83153

(b) Model with 20° leading-edge droop and 15-percent chord-extension.

Figure 1.- Concluded.

L-1060

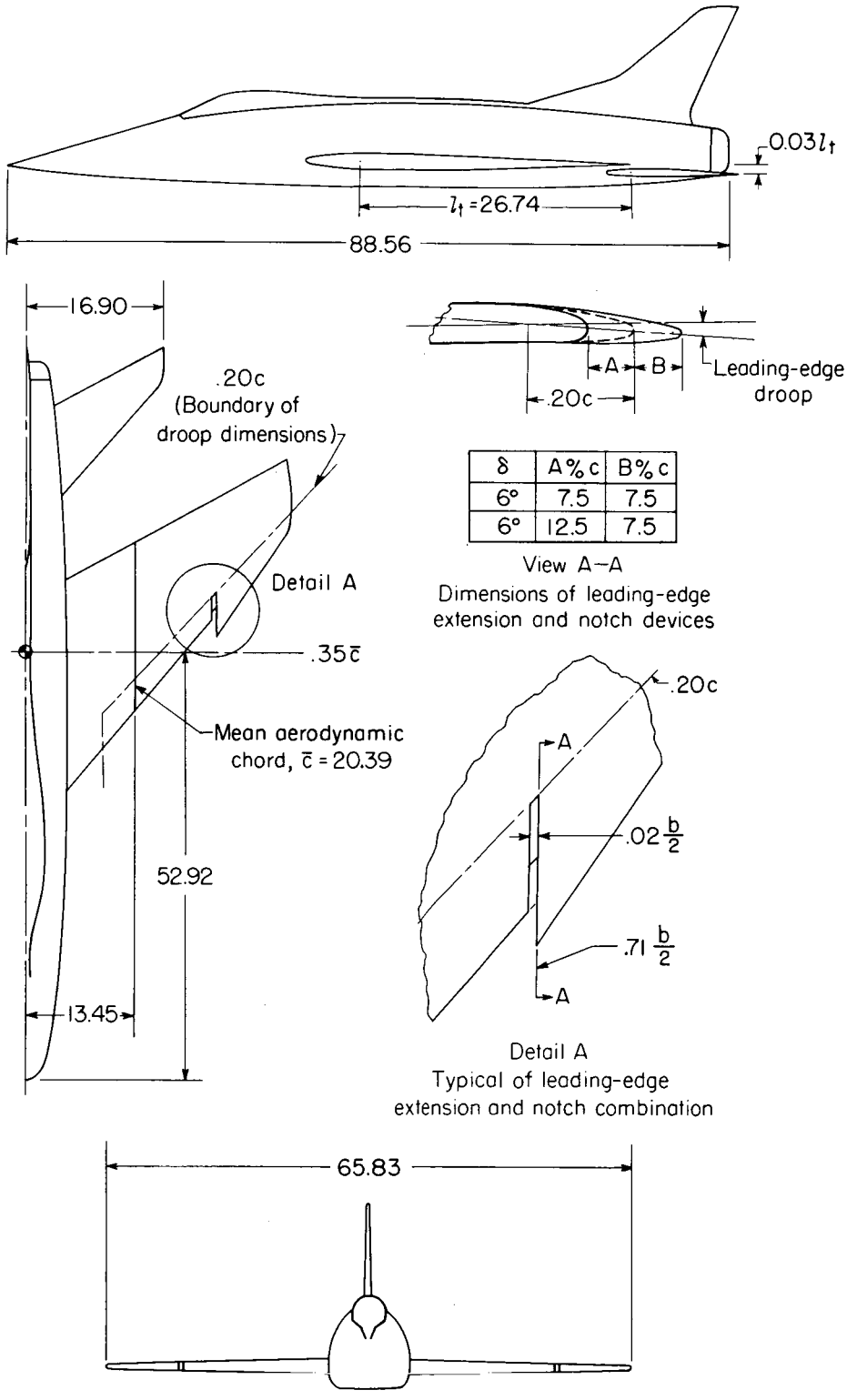

δ	A % c	B % c
6°	7.5	7.5
6°	12.5	7.5

Figure 2.- Three-view drawing of model tested.

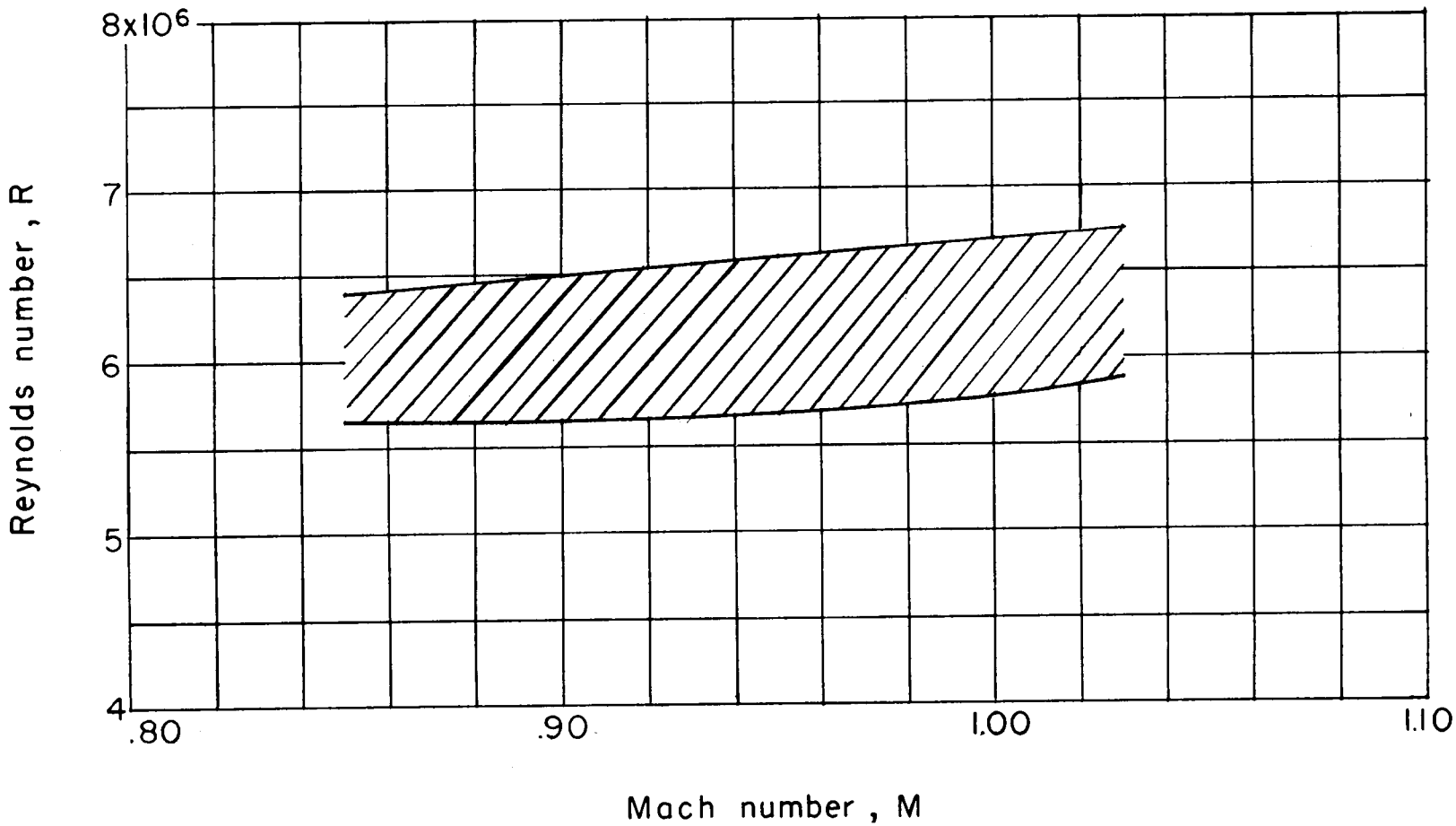

Figure 3.- Variation of Reynolds number with Mach number based on $\bar{c}$ = 1.699 feet.

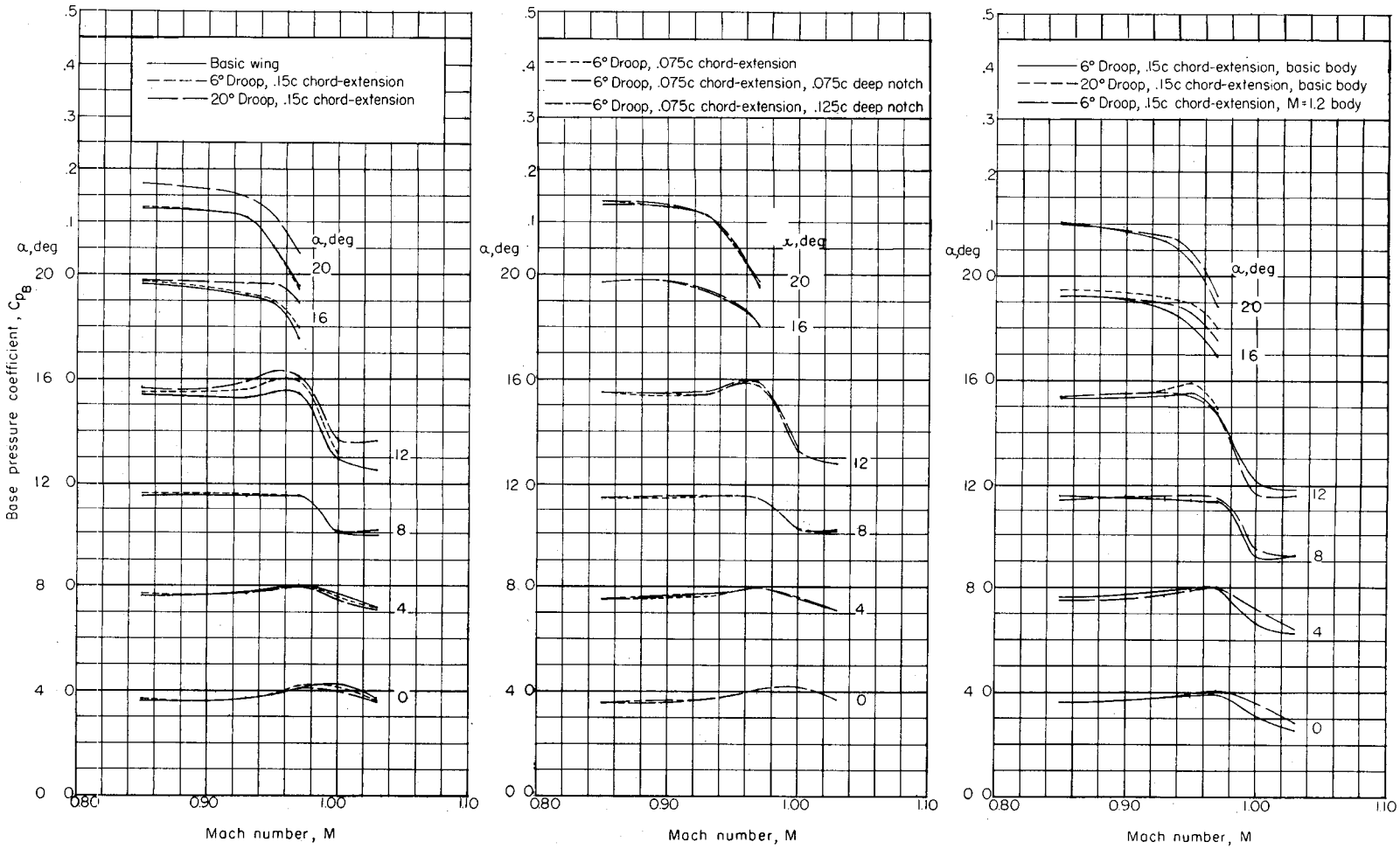

(a) Tail off. (b) Tail off. (c) Tail on, $\delta_h = -5^\circ$.

Figure 4.- Base pressure coefficients obtained with various model configurations.

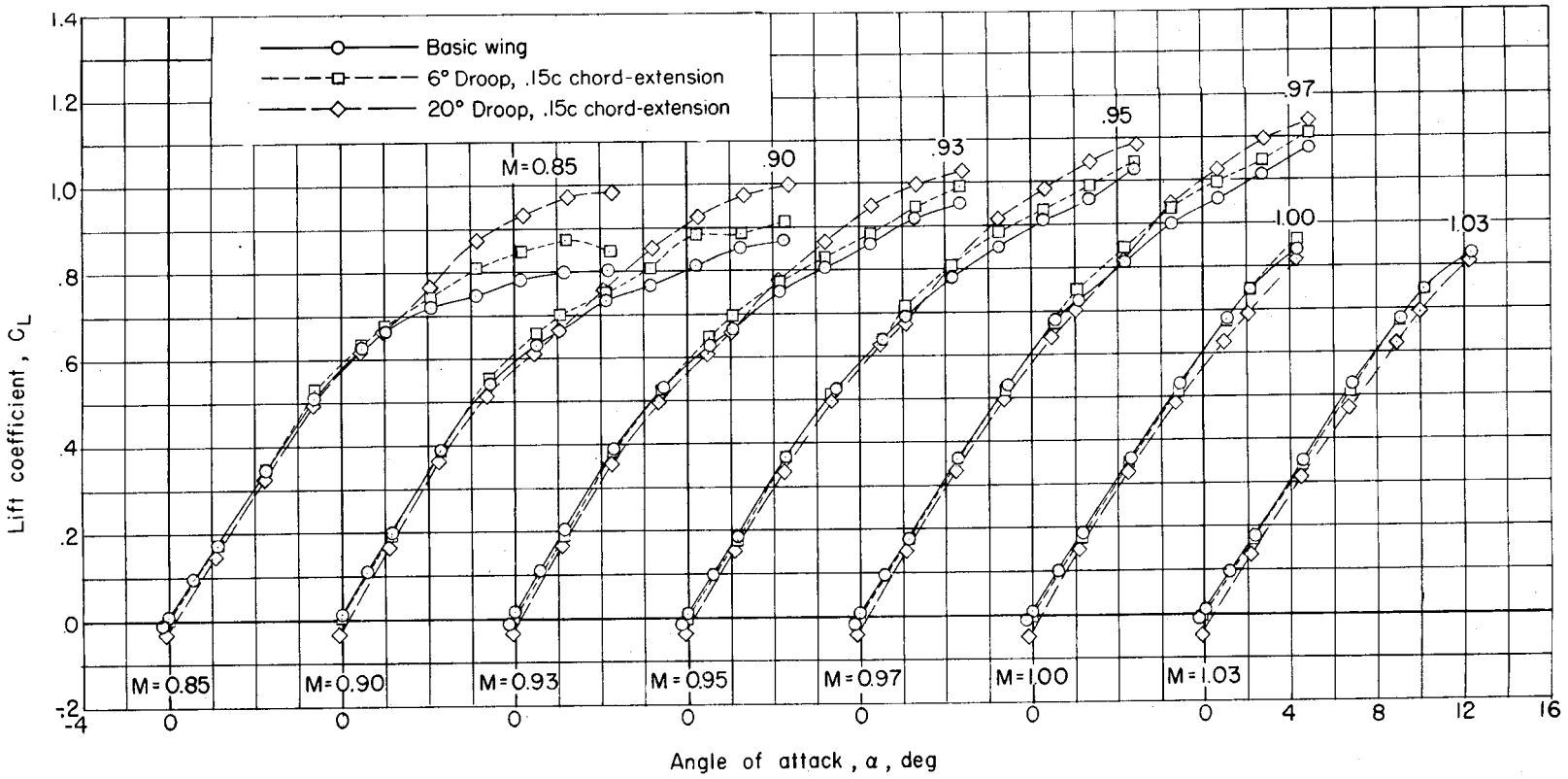

(a) Lift characteristics.

Figure 5.- Aerodynamic characteristics of tail-off configurations showing effects of leading-edge droop in conjunction with chord-extensions.

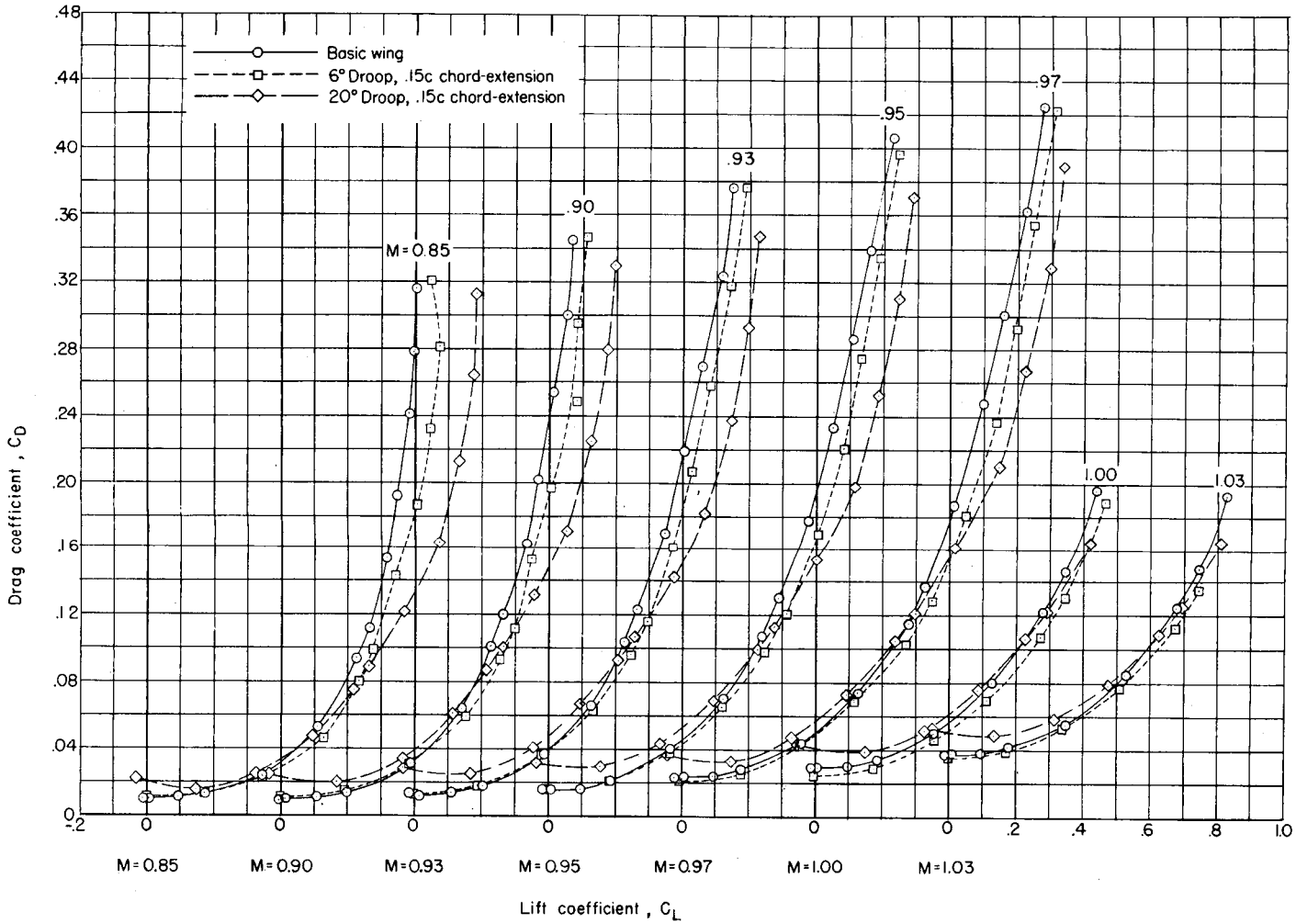

(b) Drag characteristics.

Figure 5.- Continued.

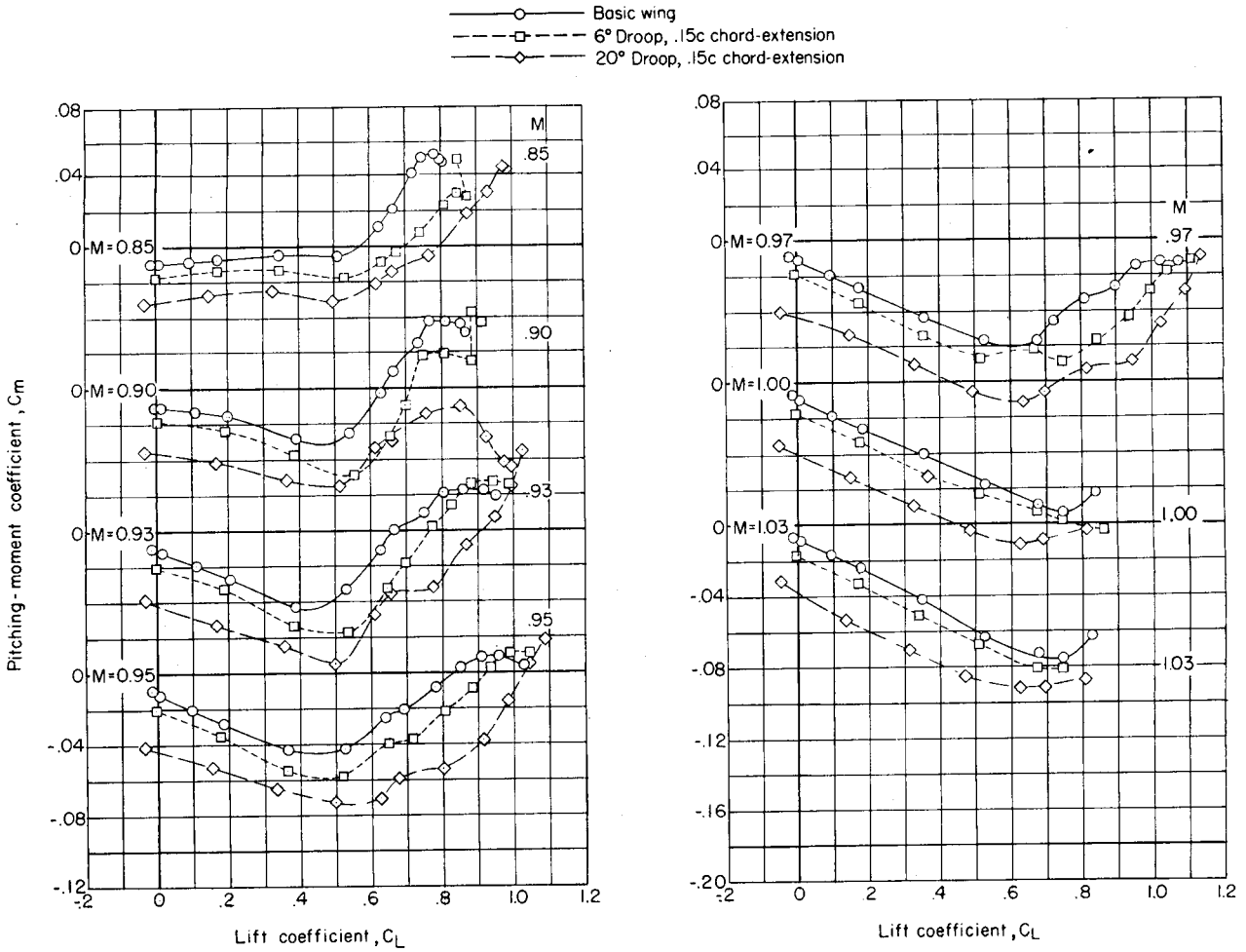

(c) Pitching-moment characteristics.

Figure 5.- Concluded.

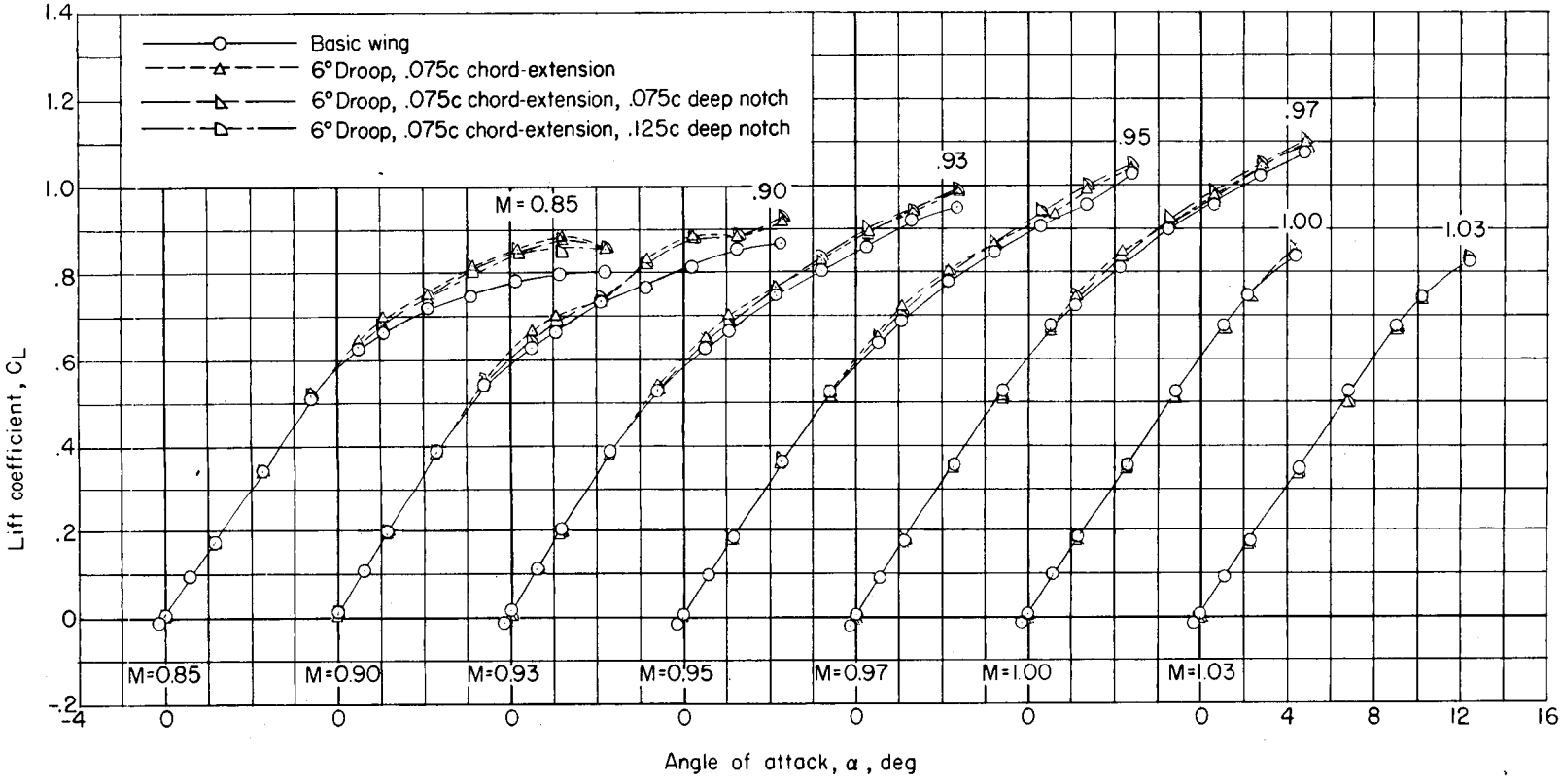

(a) Lift characteristics.

Figure 6.- Aerodynamic characteristics of tail-off configurations showing effects of 6° drooped 0.075c chord-extension with notches.

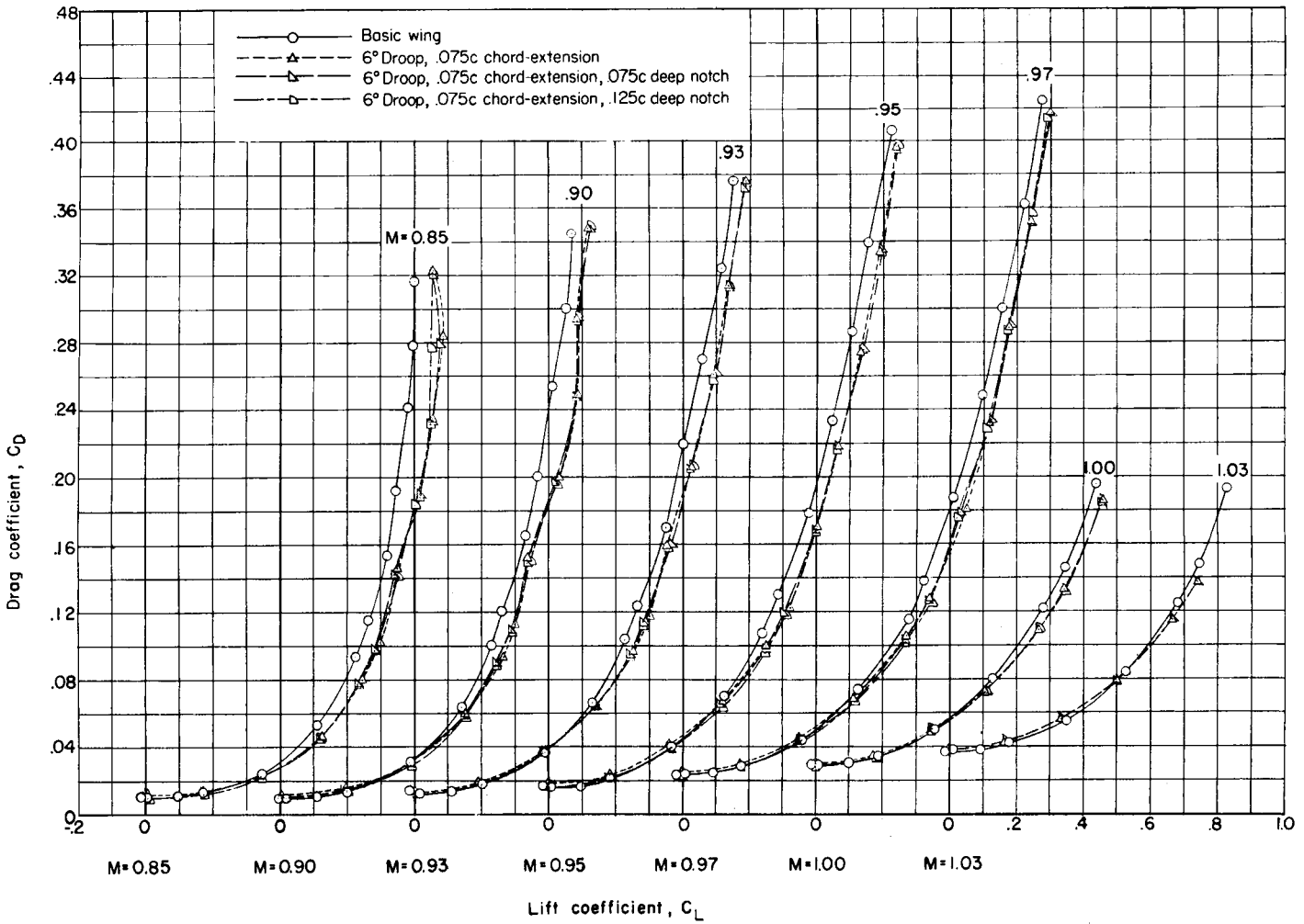

(b) Drag characteristics.

Figure 6.- Continued.

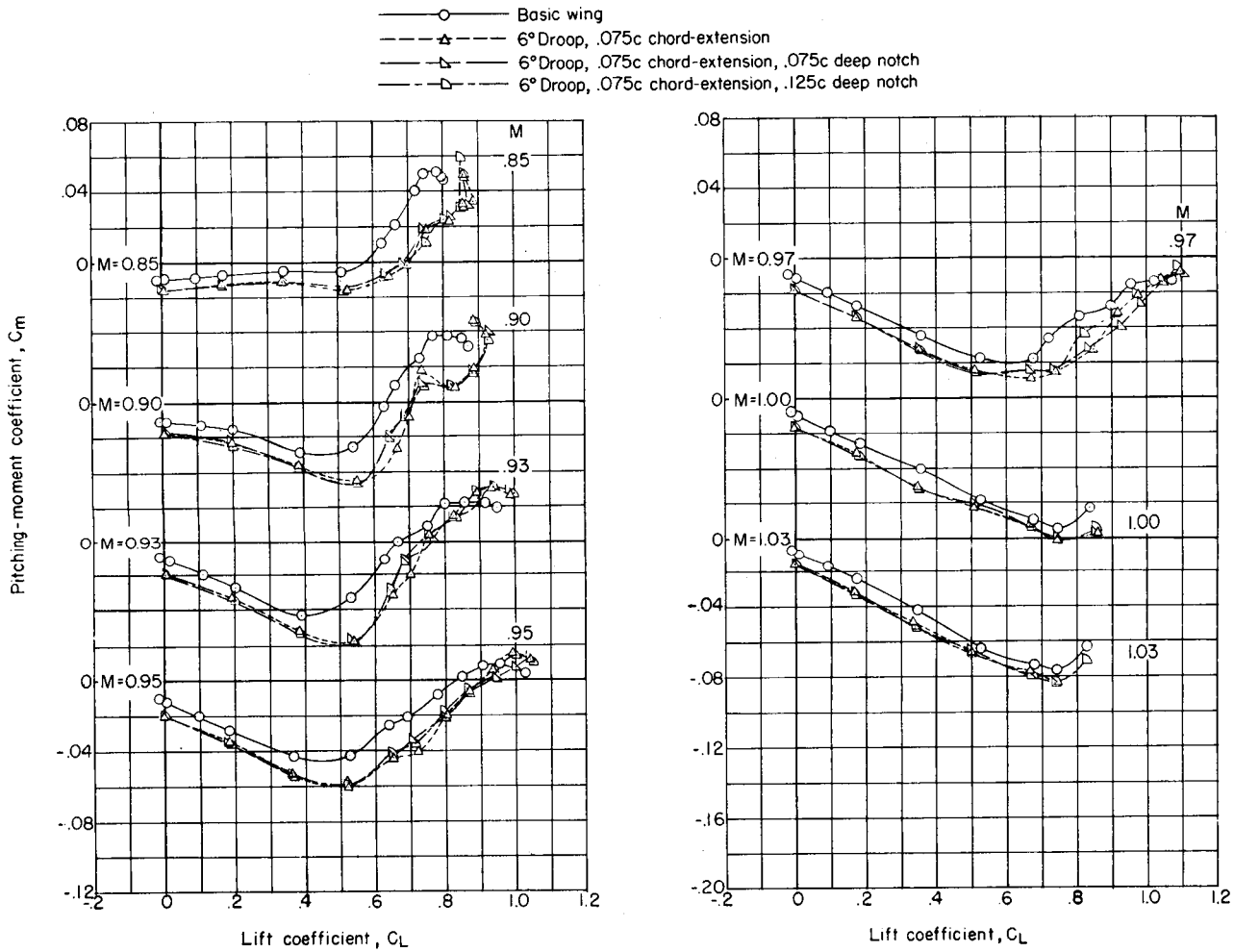

(c) Pitching-moment characteristics.

Figure 6.- Concluded.

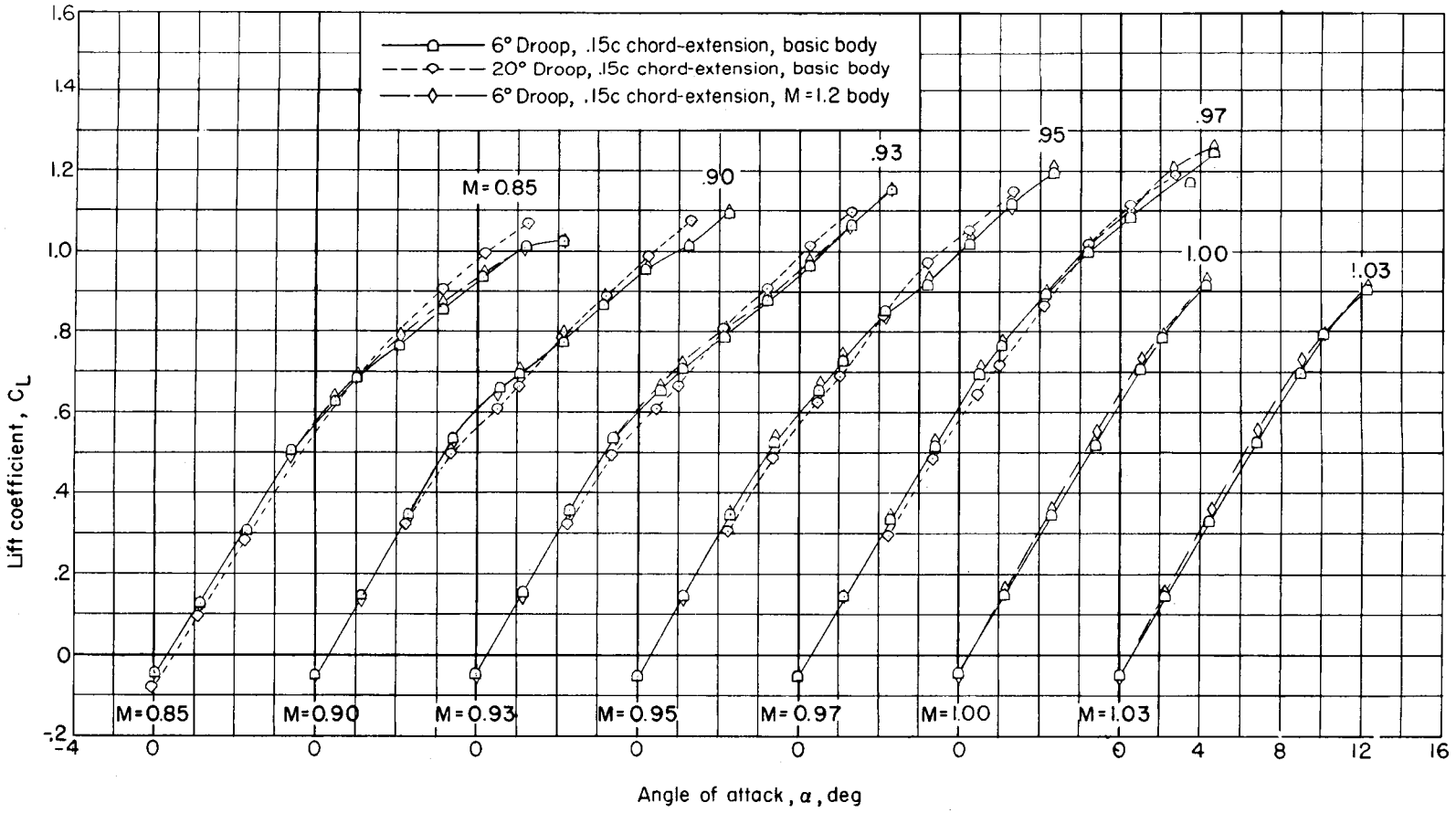

(a) Lift characteristics.

Figure 7.- Aerodynamic characteristics of tail-on configurations; $\delta_h = -5^{\circ}$.

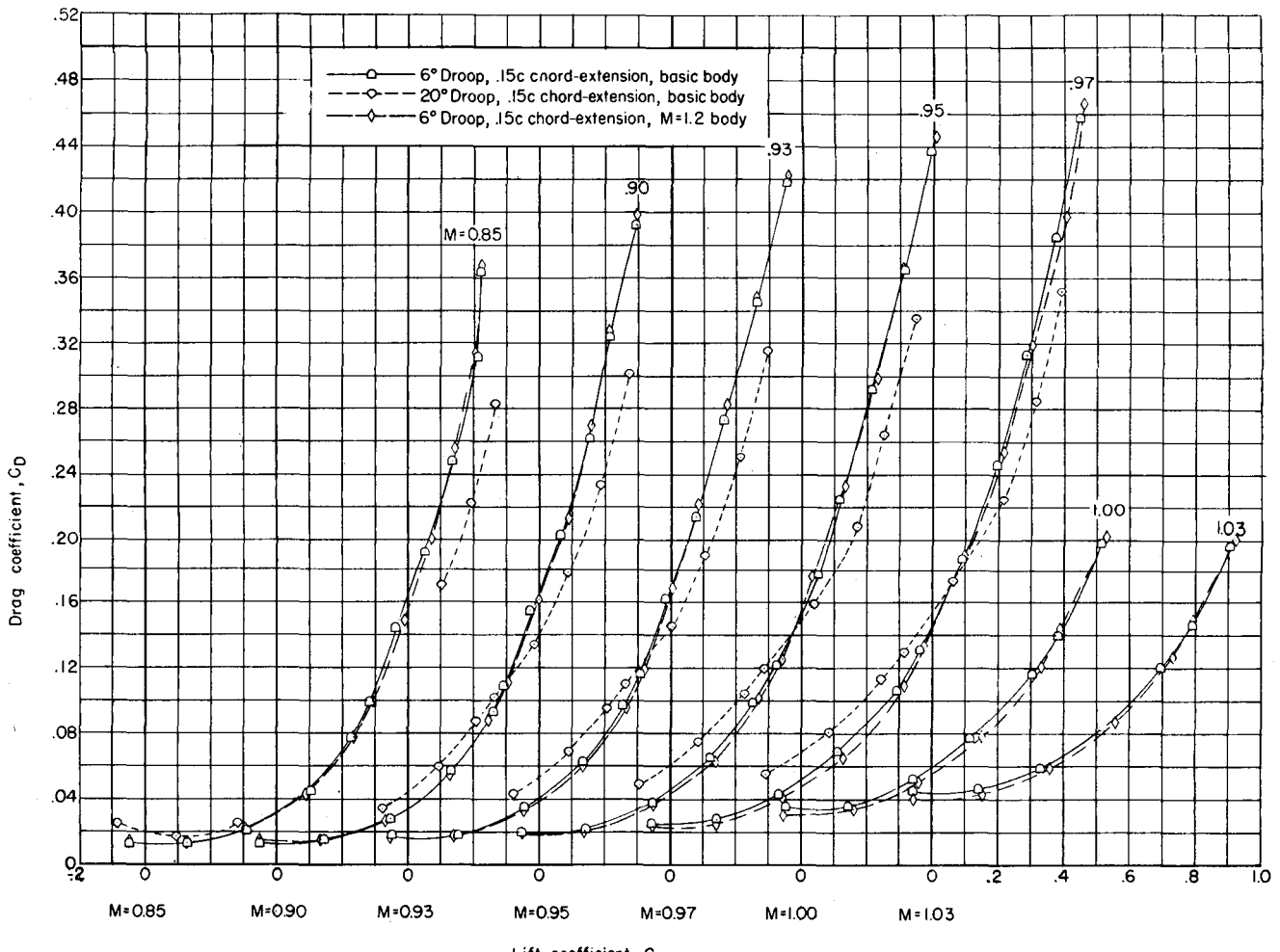

(b) Drag characteristics.

Figure 7.- Continued.

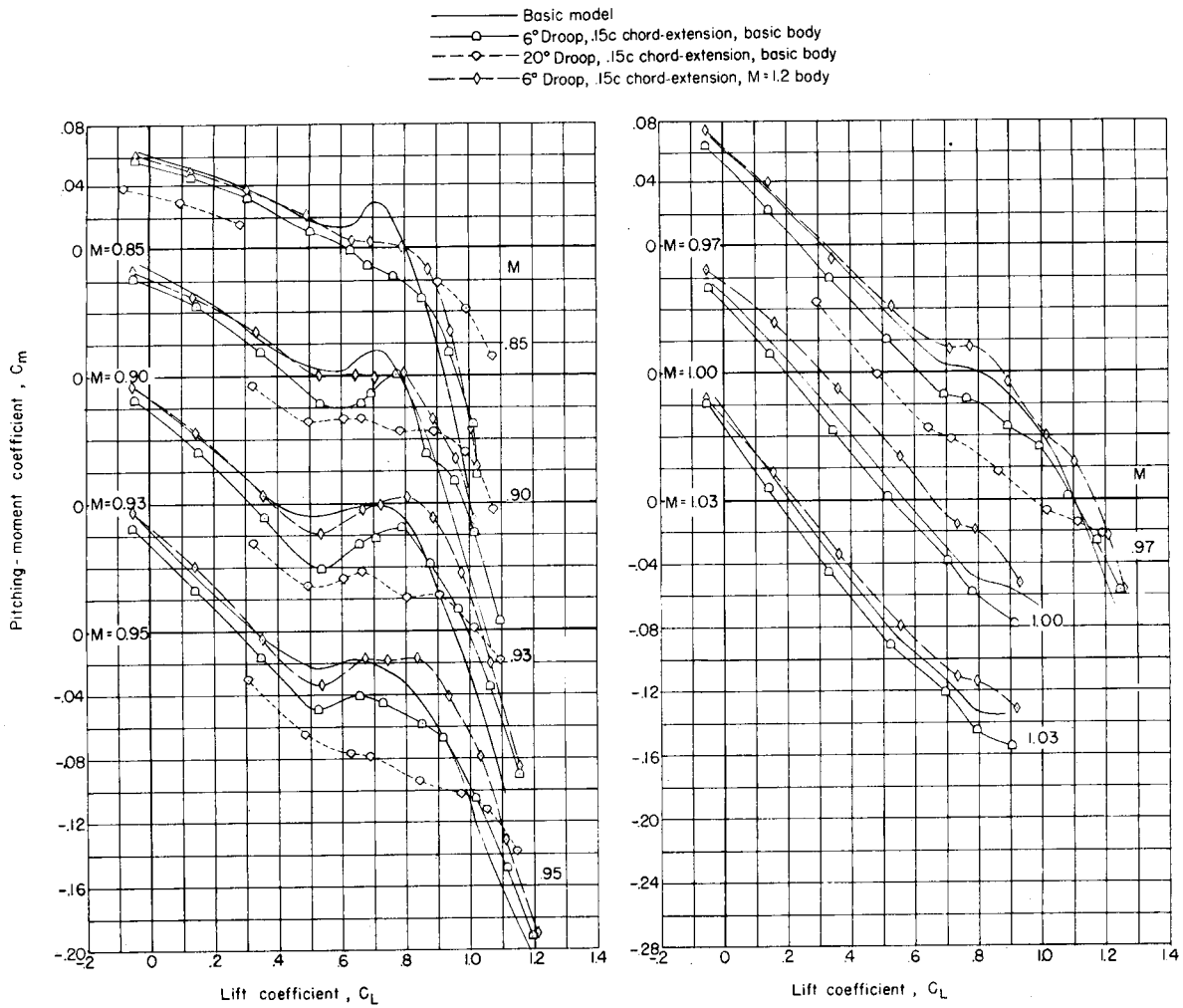

(c) Pitching-moment characteristics.

Figure 7.- Concluded.

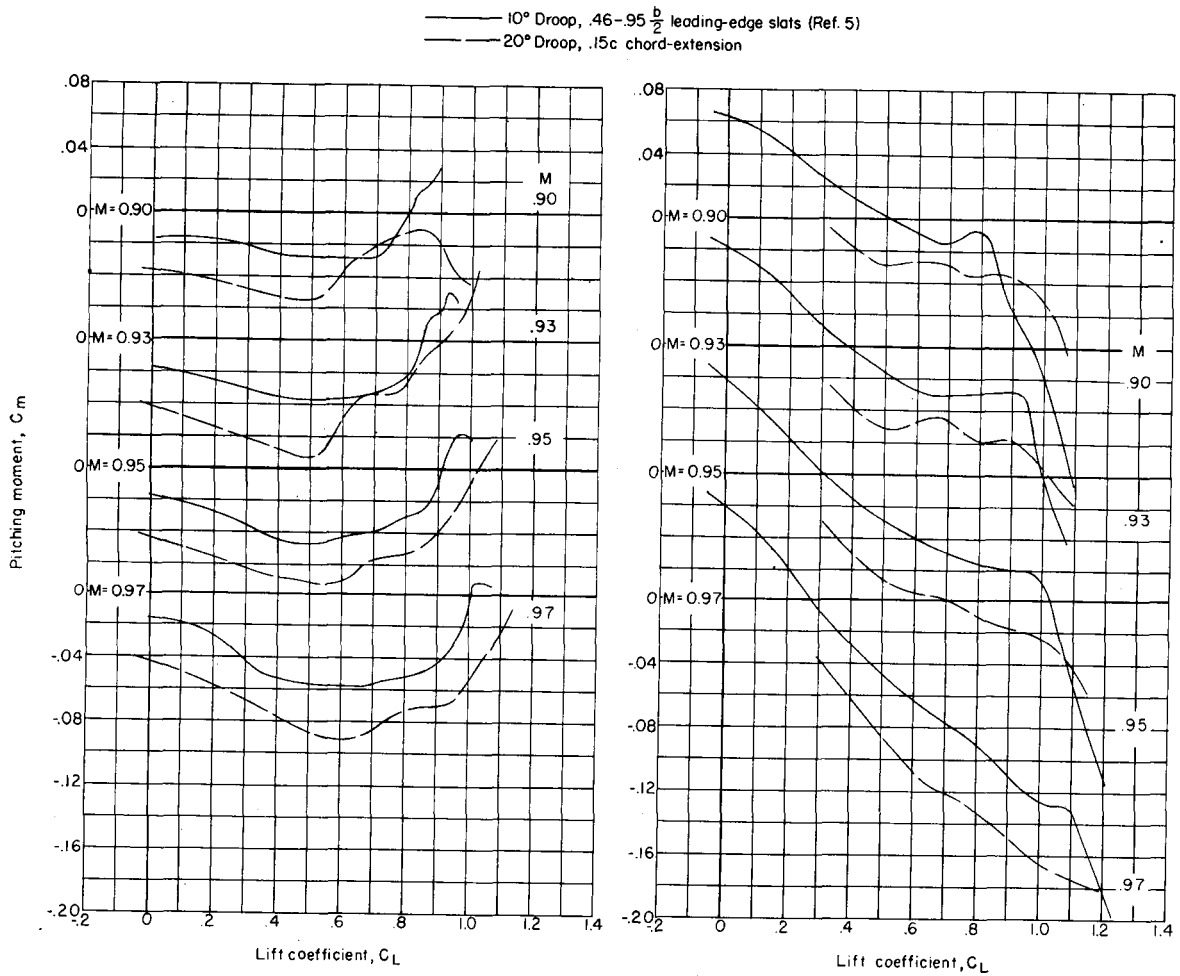

(a) Tail off.

(b) Tail on; $\delta_h = -5^\circ$.

Figure 8.- Variation of the model pitching-moment coefficient with lift coefficient when modified with two types of leading-edge devices.

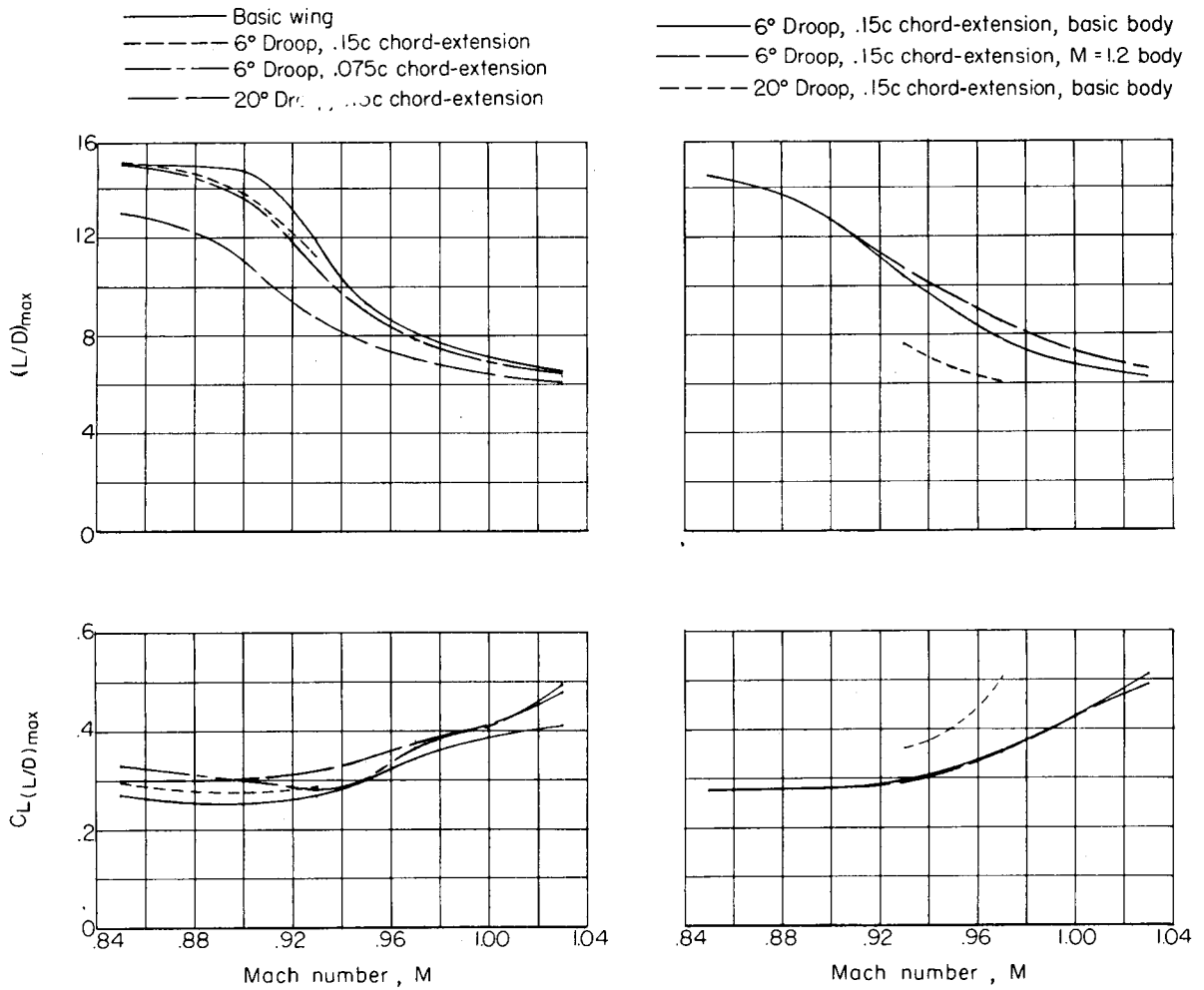

(a) Tail off.

(b) Tail on; $\delta_h = -5^{\circ}$.

Figure 9.- Effect of Mach number on $(L/D)_{max}$ and lift coefficient for $(L/D)_{max}$ for several tail-on and tail-off configurations.

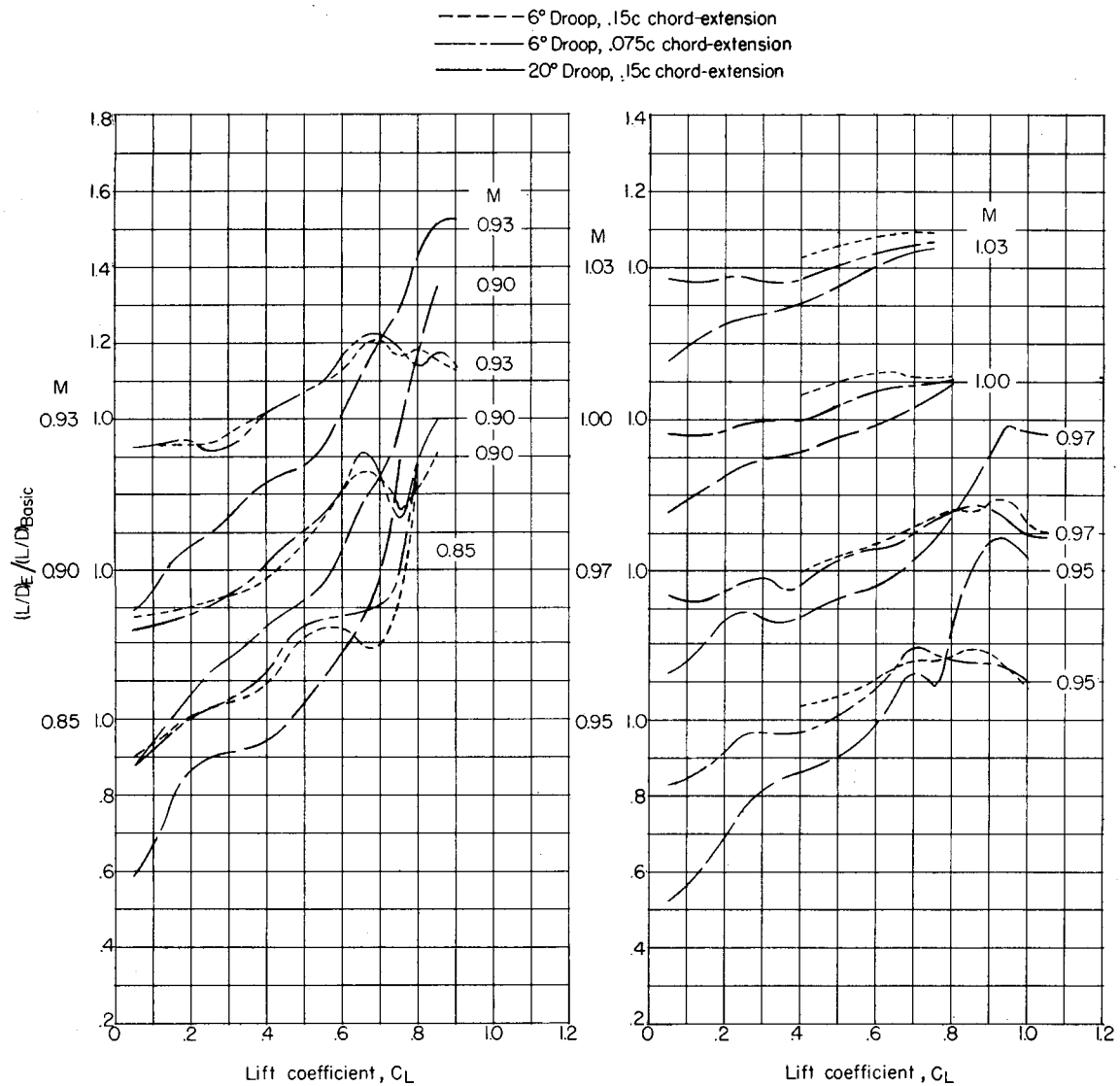

Figure 10.- Variation with lift coefficient of the ratio of L/D for several of the configurations with drooped chord-extensions to L/D for the basic model; tail off.

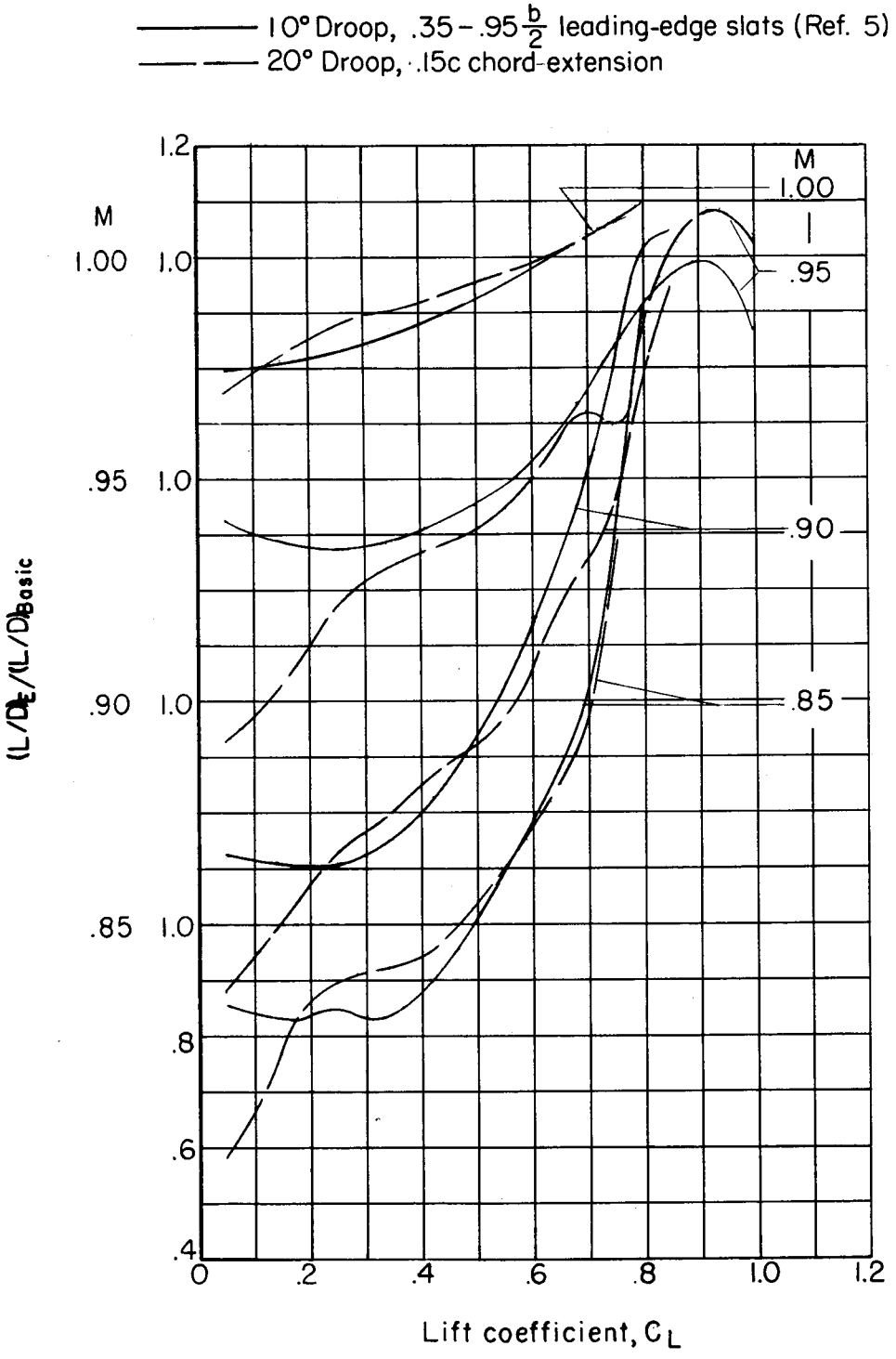

Figure 11.- Variation with lift coefficient of the ratio of L/D for two different leading-edge-device configurations and L/D for the basic model; tail off.